JOURNAL OF OPTOELECTRONICS AND ADVANCED MATERIALS, Vol. 10, No. 9, September 2008, p. 2187 - 2191

Invited Paper

NMR in solid ionics and nanoionics

D. INKMANN
Physik-Institut, University of Zürich, CH-8057 Zürich, Switzerland

The paper revues some typical NMR experiments performed in solid ionics together with some examples from nano-ionics: (i) magic angle spinning, (ii) spin-echo double resonance; (iii) measurement of the diffusion coefficient; (iv) quadrupolar effects; (v) spin-lattice relaxation.

(Received February 25, 2008; accepted August 14, 2008)

Keywords: Solid state ionics, Nanoionics, NMR

1. Introduction

"Solid State Ionics" is a research discipline dealing with solid electrolytes (also called "superionic conductors") which are solids whose conductivity is comparable to that of liquid electrolytes. Since it is an interdisciplinary subject involving chemistry, physics, and material sciences, solid state ionics research comprises many methods, among these Nuclear Magnetic Resonance (NMR). This paper revues some typical NMR experiments performed in solid electrolytes, starting around 1975 when a new interest arose in solids with high ionic conductivity

2. Line narrowing and chemical shift

NMR is a spectroscopic technique which employs magnetic nuclei to study, among others, the dynamics of a condensed matter sample at the molecular level. In principle, the NMR experiment is the observation of the nuclear Zeeman effect, that is the splitting of the magnetic energy levels of magnetic nuclei in a static magnetic field. A radio-frequency field applied at the proper frequency, induces transitions between these levels and gives rise to an NMR signal at a certain frequency ν. From these signals one deduces information on static and dynamic properties of the solid electrolyte at its molecular level.

For nuclei with a nuclear spin 1/2 (*e.g* ^{1}H, ^{19}F, ^{31}P, ^{107,109}Ag), the NMR frequency, ν, measured in an *external* static magnetic field, B_0, is given by $2\pi\nu=\omega=\gamma(B_0+\Delta B)$. Here, γ is the gyromagnetic ratio, which has a unique value for each magnetic isotope, and ΔB is an additional *local* field. ΔB arises from electric currents induced by B_0 in the electron cloud of the molecule under investigation. Since $\Delta B \sim B_0$, the resonance equation may be re-written as $\omega=\gamma B_0(1-\sigma)$, where $\sigma=-\Delta B/B_0$ is the shielding or screening constant of the order 10^{-6} to 10^{-5}. Since σ depends on the chemical environment, the frequencies of NMR signals of the same isotope in *different* compounds or in *inequivalent* sites of the same compound are shifted against each other. This effect is called chemical shift which is of fundamental importance for the chemical structure analysis by NMR.

Besides ΔB, there are other fields which contribute to the final linewidth of the NMR signal, especially the static and dynamic magnetic fields arising from all surthe rounding nuclei and atoms. At sufficient high temperatures, the fast ion movements average out, to a certain extent, these fluctuating local magnetic fields and reduce the linewidth; this effect is known as *motional narrowing*. There are two limiting cases: the ion under consideration is mobile in a more or less stationary surrounding or the ion is stationary and its neighborhood is mobile, for instance because of diffusing ions or rotating molecules.

In the absence of any motion, that is at sufficiently low temperatures, one observes the rigid-lattice linewidth, $\Delta\nu_{RL}$. If the temperature is gradually increased, the linewidth, $\Delta\nu$, decreases in a smooth step and reaches, at sufficiently high temperature, a limiting value, the residual linewidth, $\Delta\nu_r$, which is due to interactions not affected by the atomic movements.

As an example, we consider $LiNbO_3$ which is not an intrinsic ionic conductor; however, ball-milling enhances the Li conduction which predominantly takes place in the amorphous phase. Consequently, the ^{7}Li signal linewidth [1] observed in the bulk is nearly temperature independent while the increased Li conductivity in the amorphous and the ball-milled phases causes a reduction of the linewidth.

3. Magic angle spinning (MAS)

In order to acquire the information about local environments, the NMR lines with different chemical shifts must be distinguished, hence they should not overlap. If the lines cannot be resolved, they must be narrowed artificially; this can, for instance, be accomplished by *magic-angle spinning* (MAS). Let us assume the magnetic moments are coupled by magnetic fields arising from their

dipole moments; this coupling contributes to the finite linewidth. The angular dependent factor of the coupling is $A = 1 - 3\cos^2\Theta_{jk}$ where Θ_{jk} is the angle between B_0 and the vector r_{jk} joining two magnetic moments j and k. We now rotate rapidly the sample about an axis which makes an angle Θ' with B_0 and an angle α_{jk} with r_{jk}. The time average of A becomes then

$$< A >= (1 - 3\cos^2\Theta')\ (1/2)(3\cos^2\alpha_{jk} - 1).$$

If we choose $\Theta' = 54^\circ 44'$, we have $<A> = 0$ and the line is narrowed.

Let us consider the room temperature ^{27}Al MAS spectra of $MgAl_2O_4$ [2]. MAS allows to distinguish different coordinations: One signal (A) corresponds to tetrahedrally coordinated Al (with a chemical shift $\delta \approx 70$ ppm) and another signal (B) to octahedrally coordinated Al ($\delta \approx 8$ ppm) in $MgAl_2O_4$. Milling results in an decrease of the Al^{3+} concentration at B sites with the decrease increasing with the length of the milling time. The concentration decrease is accompanied by a slight change of the chemical shift and a broadening of the spectra. This change of the local environment of the Al ions is explained as a results of the deformation of both the Al tetrahedra and octahedra due to milling.

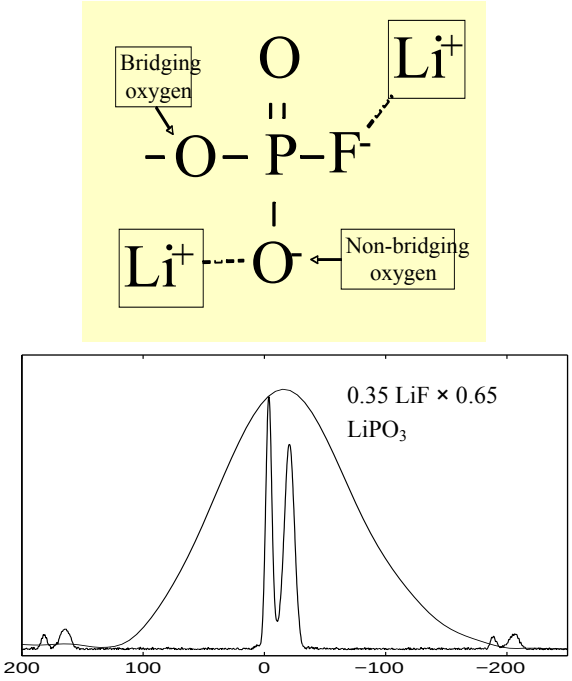

Fig. 1. Left: Structural unit of xLiF×(1-x)LiPO$_3$. Right: Broadline and MAS (the central peaks) ^{31}P spectra at 300 K and 81 MHz. Abscissa: δ in ppm.

The next example concerns a superionic glass, namely 0.35 LiF × 0.65 $LiPO_3$ [3]. This is an important electrolyte because of its wide range of anion substitution and the large variety in composition. The compound consists of PO_4 tetrahedra (see Fig.1) with P in the center, which are interconnected via bridging O ions, thus forming a glassy network. F atoms are embedded in the glassy structure preferentially by substituting bridging O ions. Thus, LiF is not only a dopant, it also modifies the network via further depolymerization, thus increasing the number of end groups. MAS separates two lines with chemical shifts of -8 ppm and -22 ppm which correspond to phosphate end and middle groups, respectively.

4. Spin-echo double resonance (SEDOR)

In the last example, the assignment of the chemical shifts to certain phosphate positions is based on the good agreement of these values with known isotropical chemical shifts in phosphate tetrahedra. A more direct "proof" of assignements is provided by a spin-echo double resonance (SEDOR) experiment. It goes as follows: One performs a spin--echo experiment on a nuclear I (at the Larmor frequency of the I spin) by the application of a $\pi/2 - \pi$ pulse sequence where the π pulse flips the spin by 180°. At a time τ_F after the start of the $\pi/2 - \pi$ sequence, one flips another spin, an S spin (at the S spin Larmor frequency). If the two nuclei involved, I and S, are physically near each other, *i.e.* if they are coupled by a spin-spin interaction, the application of the π pulse to the S spin will disturb the I spin--echo, which is now reduced. The decay of the SEDOR signal is described by

$$E_{SEDOR}(2\tau_F) = E_{SO}\ \exp\left[(-1/2)(2\tau_F / T_{SEDOR})^2\right]$$

where T_{SEDOR} is the decay time constant.

In the case of 0.35 LiF × 0.65 $LiPO_3$, we were interested in the assignment of the NMR lines in the ^{19}F spectrum. I and S stand now for the ^{31}P and ^{19}F nuclear spins, respectively. The much stronger echo decay of one ^{19}F line immediately shows that the corresponding F ions are closest to the phosphorus nuclei. Hence, this line has to be assigned to F ions in PO_3F tetrahedra while the other two lines are due to F ions in Li^+F^- fragments which are more distant to the central phosphorus atom of the PO_4 tetrahedra.

5. Diffusion coefficient

Skejskal and Tanner [4] invented the *pulsed-field gradient* (PFG) technique which is an elegant method to measure the diffusion coefficient, D, in a model independent way. In its simplest version (see Fig. 2), the method employs the Hahn $\pi/2 - \pi$ spin-echo experiment mentioned in the previous chapter. In addition, a magnetic field gradient pulse is applied after each radio-frequency (*rf*) pulse. These gradients "label" the diffusing ions by their respective Larmor frequency. In the absence of diffusion, the effects of G_1 and G_2 cancel. However, if spins change their spatial position between the application

of the gradient pulses, the spin-echo signal will be attenuated. If one measures the echo amplitudes A_G and A with and without gradient pulses, respectively, the diffusion coefficient D_{NMR} follows from the relation [4]

$$\ln(A_G / A) = \gamma^2 D_{NMR} \delta^2 [\Delta - (1/3)] g^2.$$

The meaning of δ, Δ, and g is given in Fig. 2. The steady background gradient is assumed to be very small with respect to *g*.

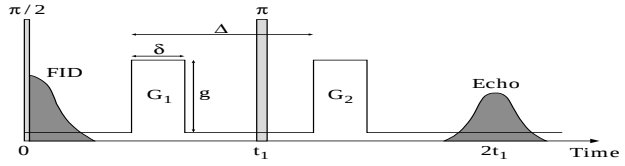

Fig. 2. Arrangement of radio-frequency (π/2,π) and field-gradient (G_1, G_2) pulses in the PFG experiment to measure the diffusion coefficient. One observes the spin-echo signal (after Fourier transformation). FID is the free-induction decay signal induced by the π/2 pulse.

The magnitude of the diffusion coefficient is a valuable information by itself. The NMR methods allow, however, to gain additional knowledge by measuring, for instance, the anisotropy of D_{NMR}, as in Li_3N and β-$LiAlSiO_4$. Further, one may combine D_{NMR} with the diffusion coefficient, D_σ, derived from conductivity measurements via the Nernst-Einstein equation. This results is the Haven ratio, $H_R = D_{NMR} / D_\sigma$, which reveals correlation effects in the ion dynamics. For instance, in the crystalline Ag conducting KAg_4I_5 and $RbAg_4I_5$ compounds, which undergo a phase transition in the superionic phase, we detected an unusually low value of H_R of about 0.5. Such values may be the result of a "caterpillar" effect; that is a cooperative motion of two or more ions in such a way that a jumping ion causes other ions to jump in the same direction. At the transition form the high- to the low-temperature phase, H_R decreases implying an increase of the number of ions involved in the caterpillar movement. In the low-temperature phase of $RbAg_4I_5$, D_{NMR} of ^{109}Ag is about 3×10^{-13} m^2/s. For comparison: the diffusion coefficient of water at 300 K is about 10^{-9} m^2/s.

While in many crystalline solid electrolytes the diffusion coefficient displays an Arrhenius temperature dependence (and thus directly yields the activation energy), the diffusion coefficient in superionic polymers quite often follows the Vogel-Tammann-Fulcher equation

$$D \cdot T^{-1/2} = A \cdot \exp[-E / k(T - T_0)].$$

In the framework of the "free-volume model", E is an apparent activation energy and T_0 is the ideal glass transition temperature at which the free volume, which is available for segmental motion, tends to zero and thus translational motion ceases.

6. Quadrupole interactions

When we are dealing with nuclei with a spin larger than ½ we may take advantage of the fact that these nuclei posses an electric quadrupole moment, *eQ*, which interacts with electric field gradients (EFG) present at the nuclear site (if its symmetry is non-cubic) and arising from all the surrounding charges. This quadrupole interaction causes the NMR signal to split (in an ordered structure) or to broaden (in "powder" samples). For instance, nuclei like ^7Li, ^{11}B, ^{23}Na, and $^{63,65}Cu$ with spin 3/2 yield a spectrum of 3 components. The separation of these lines depends on the strength of eQ and the EFG and on the orientation of the EFG tensor with respect to the magnetic field. Since the NMR frequencies are very sensitive to even minor changes of the EFG, nuclei of the same isotope but located at inequivalent sites are easily distinguished: they yield different triplets.

These quadrupole effects may be a gold mine for structural and dynamical studies of solid electrolytes. The EFG reflects any slight rearrangement of charges in the neighborhood of the nucleus under investigation. Thus, quadrupole effects are the ideal tool to investigate, among others, structural phase transitions, the changes of the atomic disorder or order (for instance at the transition from a high- to a low-conducting phase), the presence of imperfections (which alter the EFG), and the nature of bonding which is associated with different charge arrangements. Since the EFG is a tensor, its symmetry reflects the local symmetry of the nuclear site.

As an example, let's look at Li_3N, which belongs to those solid electrolytes most exhaustively studied by NMR [5,6]. Li_3N is a layer-structure with different NMR spectra for the inter-layer Li(1) and the intra-layer Li(2) nuclei. Increasing the temperature enhances the ion exchange between the two inequivalent sites; finally, at about 600 K, this process is so rapid that one observes only an "averaged" triplet. The exchange process has been monitored by the temperature dependence of several NMR parameters: the quadrupole shift (with respect to the NMR frequency in the case of zero EFG), the spin-lattice relaxation (see next section), and the diffusion coefficient. They all yield the same temperature dependent Li hopping frequencies thus supporting the ion exchange model. This is an instructive example for the necessity to perform comprehensive NMR experiments in order to establish the validity of a microscopic model.

7. Spin-lattice relaxation

One of the unique powers of NMR is the ability to study the dynamics in a solid at the molecular level by performing relaxation experiments. Here, we will restrict ourselves to nuclear spin-lattice relaxation which is the

process how a nuclear spin system approaches thermodynamic equilibrium with the lattice, by which we mean all the other degrees of freedom in the sample, beside the nuclear spins. The time constant of this process is called spin-lattice relaxation time, T_1. In simple cases, the relaxation is brought about by local magnetic fields fluctuating at the Larmor frequency and inducing transitions in the spin system. If the correlation function, G(t), of these fluctuations is known, one can extract, from the data analysis, motional correlation times, τ, which are related to microscopic processes such as diffusion of ions and vacancies, moving defects, molecular rotations etc.

In the early days of NMR, relaxation data were analyzed by making the simple assumption of an exponential correlation function: $G(t) = G(0) \cdot \exp(-t/\tau)$. A Fourier transform of *G(t)* leads to the spectral density function and then to the well-known Bloembergen-Purcell-Pound (BPP) formula for the spin-lattice relaxation rate:

$$\frac{1}{T_1} = C^2 \left[\frac{\tau}{1+(\omega_0 \tau)^2} + \frac{4\tau}{1+(2\omega_0 \tau)^2} \right],$$

where *C* is a measure of the strength of the fluctuating local field. One often assumes, for τ, an Arrhenius behavior and identifies τ with the thermally activated mean residence time of jumping ions. The data then yield the activation energy, *E*, and the attempt frequency, $1/\tau_0$, of the atomic process.

The BPP formalism works quite well for gases, liquids, and several solids and it has been applied in several areas of solid state physics. In many solid electrolytes, however, it is only qualitatively correct since these compounds are many-particle systems which are not properly accounted for by an exponential correlation function. Here, we will mention two simple extensions of the BBP formula.

The first example is the consideration of a *temperature* dependent concentration of vacant sites in solid electrolytes. In Li_3N, vacancy-induced diffusion allowed us to interpret the temperature and orientation dependent T_1 values of both ^{7}Li and ^{6}Li. The ansatz for the concentration of vacant Li sites is as follows:

$$c(T) = c_0 + c_0' \exp(-E_{fv}/kT)$$

c_0 is the temperature independent concentration, *c_0'* is an appropriate prefactor, and E_{fv} is the formation enthalpy for vacancies. The analysis of the data yields $c \approx 2$ %; this result was confirmed much later by x-ray studies.

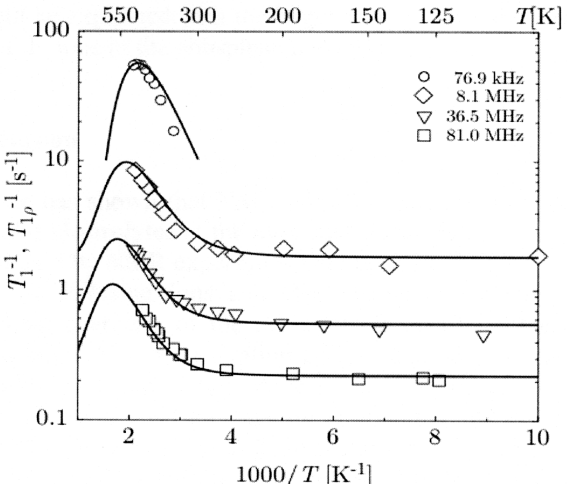

Fig. 3. Temperature dependence of the ^{31}P relaxation times in the laboratory frame (MHz range, T_1) and in the rotating frame ($T_{1\rho}$) at various frequencies in x LiF (1-x) $LiPO_3$..

In our second example, we consider again the phosphate glass x LiF (1-x) $LiPO_3$. We are now interested in the relaxation of the stationary P ions [7] and we will pay attention to the inherent disorder of the glass. The disordered structure results in a distribution of bond-lengths and -angles which can be taken into account by assuming a Gaussian distribution of activation energies with a center E_0 and half width ΔE.

The formulae for the relaxation times in the laboratory frame, T_1, and in the rotating frame, $T_{1\rho}$, were fitted to the corresponding experimental data *simultaneously* over the whole frequency range from several kHz to 81.0 MHz. The result for 0.35 LiF × 0.65 $LiPO_3$ is: E_0 = 0.72 eV, ΔE = 0.143 eV, $\tau_0 = 0.94\ 10^{-13}$ s. For $LiPO_3$, we obtain E_0 = 0.817 eV. For both samples, our E_0 values surprisingly well compare with activation energies obtained by DC conductivity measurements. This agreement is not trivial, since DC conductivity cannot reflect details of an activation energy distribution as the microscopic NMR method does. The increase of ΔE with doping might be explained with the larger variety of Li sites due to the incorporation of F ions in the phosphate network.

8. Conclusion

Our revue has shown that NMR allows to acquire a wealth of information about solid electrolytes at the molecular level. We list some other information obtained by NMR experiments but not discussed here: (1) the kind and number of diffusing ions and their diffusion pathways (one- or two-dimensional character of the motion); (2) details of the ion hopping frequencies like prefactor, activation energy, and activation volume (via pressure studies); (3) correlation effects and cooperative phenomena of

these motions; (4) local symmetry, nature of bonding, and imperfections; (5) order-disorder phenomena and phase transitions. For further details we refer to Ref. [6]. As to nanoionics, we believe that NMR will contribute to the understanding of these materials in a similar way as we have seen in solid electrolytes.

References

[1] A. V. Chadwick, S. L. P. Savin, Solid State Ionics **177**, 3001 (2006).
[2] V. Šepelac, S. Indris, I. Bergmann, A. Feldhoff, K. D. Becker, P. Heitjans, Solid State Ionics, **177**, 2487 (2006).
[3] St. Berger, J. Roos, A. Yu. Zavidonov, D. Brinkmann, Solid State Ionics **112**, 87 (1998).
[4] E. O. Stejskal, J. E.,Tanner, J. Chem. Physics **42**, 288 (1965).
[5] D. Brinkmann, M. Mali, J. Roos, R. Messer, H. Birli, Phys. Rev. B **26**, 4810 (1982).
[6] D. Brinkmann, Progress in NMR Spectroscopy **24**, 527 (1992).
[7] D. Brinkmann , in: Solid State Ionics - Science & Technology ,eds. Chowdari, B.V.R., Lal, K., Agnihotry, S.A., Khare, N., Sekhon, S.S., Srivastava, P.C., S. Chandra, S., World Scientific, (Singapore) 1998, p. 93.

*Corresponding author: Detlef.Brinkmann@physik.unizh.ch